Neurochemistry International 129 (2019) 104489

Contents lists available at ScienceDirect

Neurochemistry International

journal homepage: www.elsevier.com/locate/neuint

The long dystrophin gene product Dp427 modulates retinal function and vascular morphology in response to age and retinal ischemia

Felicitas Bucher[a,b], Mollie S.H. Friedlander[a], Edith Aguilar[a], Toshihide Kurihara[a], Tim U. Krohne[a], Yoshihiko Usui[a], Martin Friedlander[a,*]

[a] Department of Molecular Medicine, The Scripps Research Institute, La Jolla, CA, 92037, USA
[b] Eye Center, Medical Center, Faculty of Medicine, University of Freiburg, Germany

ARTICLE INFO

Keywords:
Duchenne muscular dystrophy
Dp427
Electroretinography
Proliferative retinopathy
Hypoxia
Angiogenesis
Oxygen-induced retinopathy

ABSTRACT

Mutations in dystrophin are the major cause of muscular dystrophies. Continuous muscular degeneration and late stage complications, including cardiomyopathy and respiratory insufficiency, dominate the clinical phenotype. Gene expression and regulation of the dystrophin gene outside of muscular tissue is far more complex. Multiple tissue-specific dystrophin gene products are widely expressed throughout the body, including the central nervous system and eye, predisposing affected patients to secondary complications in non-muscular tissues. In this study, we evaluated the impact of the full-length dystrophin gene product, Dp427, on retinal homeostasis and angiogenesis. Based on the clinical case of a Duchenne muscular dystrophy (DMD) patient who developed severe fibrovascular changes in the retina in response to hypoxic stress, we hypothesized that defects in Dp427 make the retina more susceptible to stresses such as ageing and ischemia. To further study this, a mouse strain lacking Dp427 expression (Mdx) was studied during retinal development, ageing and in the oxygen-induced retinopathy (OIR) model. While retinal vascular morphology was normal during development and ageing, retinal function measured by electroretinography (ERG) was slightly reduced in young adult Mdx mice and deteriorated with age. Mdx mice also had increased retinal neovascularization in response to OIR and more pronounced long-term deterioration in retinal function following OIR. Based on these results, we suggest that DMD patients with a mutation in Dp427 may experience disturbed retinal homeostasis with increasing age and therefore be prone to develop excessive retinal neovascular changes in response to hypoxic stress. DMD patients in late disease stages should, thus, be regularly examined to detect asymptomatic retinal abnormalities and prevent visual impairment.

1. Introduction

Duchenne muscular dystrophy (DMD) affects 1 out of 7200 boys aged 5–24 years in the US (Romitti et al., 2015). The disease is characterized by progressive weakness of skeletal muscles, followed by cardiomyopathy and respiratory insufficiency as the disease progresses. Improvement in overall medical care has greatly increased life expectancy for DMD patients in recent years. With increased life expectancy, new secondary complications like vasoproliferative retinopathy have become more prevalent (Louie et al., 2004). These complications indicate that DMD has a broad phenotypic spectrum due to tissue-specific dystrophin gene expression that is still not well understood.

With 2.5 million base pairs and 86 exons, the dystrophin gene is the largest gene in the human body (for review see Muntoni et al., 2003). Mutations affecting the full-length muscular dystrophin gene product, Dp427, are the major cause for progressive muscle degeneration and weakness in DMD patients. However, tissue-specific and internal promotors give rise to multiple dystrophin gene products named by their molecular weight. Dp427 (full-length dystrophin) is predominantly expressed in skeletal and cardiac muscle cells. In contrast, Dp260 is highly expressed in the retina (D'Souza et al., 1995; Pillers et al., 1993), Dp140 in brain, retina and kidney (Lidov et al., 1995), Dp116 in peripheral nerves (Byers et al., 1993) and Dp71 in most non-muscular tissues (Lederfein et al., 1992). In the retina, Dp427 and Dp260 have been shown to localize to the first synapse (Wersinger et al., 2011), while Dp71 was associated with retinal angiogenesis and vascular permeability due to its expression in perivascular Müller cell endfeet (Dalloz et al., 2003; Howard et al., 1998).

In the past, pigmentary fundus changes and varying degrees of

* Corresponding author. 10550 N Torrey Pines Rd, MB-10, CA, USA.
E-mail address: friedlan@scripps.edu (M. Friedlander).

https://doi.org/10.1016/j.neuint.2019.104489
Received 29 November 2018; Received in revised form 8 June 2019; Accepted 10 June 2019
Available online 11 June 2019
0197-0186/

electroretinographic (ERG) abnormalities depending on the site of the dystrophin mutation have been the only ocular manifestations in DMD patients (Pillers et al., 1999a; Sigesmund et al., 1994). Accumulating case reports now also suggest that DMD patients in advanced disease stages with cardio-respiratory insufficiency may be prone to development of vasoproliferative retinopathy (Fagan et al., 2012; Hahn et al., 2013; Louie et al., 2004). All published cases have, however, focused on clinical presentation and treatment options, leaving it to speculation as to whether the observed vascular changes were aggravated by defects in the dystrophin gene or purely caused by the accompanying cardio-respiratory insufficiency.

In this study, we investigate the contribution of the long dystrophin gene product Dp427 to retinal health and disease using clinical and preclinical approaches. We present a case report of a DMD patient who developed excessive proliferative retinopathy. We then use the Mdx mouse model, one of the best-studied DMD mouse models, to evaluate the impact of Dp427 on retinal development, senescence and retinal vascular disease in a preclinical setting.

2. Material and methods

2.1. Clinical data

Procedures involving human subjects were performed in accordance with the Helsinki Declaration of 1975, as revised in 1983. The male DMD patient was 21 at the time of initial presentation. Genetic analysis of the DMD gene was performed on a blood sample through MLPA analysis by the Division of Pathology, City of Hope, Southern CA. OCT imaging was performed using a Heidelberg Spectralis OCT. Fundus images were taken with a Topcon fundus camera.

2.2. Animal studies

Mice used in these studies were treated according to the NIH Guide for the Care and Use of Laboratory Animals. Performed animal studies were reviewed and approved by the IACUC of The Scripps Research Institute. The mouse model for DMD, C57BL/10ScSn-*Dmd*^{mdx}/J (Mdx), was purchased from The Jackson Laboratory. Mice were bred with corresponding wildtype controls (C57BL/10ScSnJ) to create litters containing homozygotes and wildtype littermate controls (WT littermate). During retinal development, pups were sacrificed at postnatal day 5 (P5). The model of oxygen-induced retinopathy (OIR) was performed as previously described (Smith et al., 1994). In brief, mice were exposed to 75% oxygen between P7 and P12 and subsequently transferred to room air. At OIR P17, the areas of vaso-obliteration (VO) and neovascularization (NV) were quantified according to well-established techniques (Banin et al., 2006; Connor et al., 2009).

2.3. Immunohistochemistry

Eyes were harvested and fixed in 4% paraformaldehyde for 40 min before the preparation of retinal flatmounts or cryosectioning. Cryosections were fixed in 100% Ethanol for 10 min. To ensure comparable staining patterns, corresponding cryosections of Mdx mice and WT littermate controls were always mounted and stained on the same glass slide. Primary antibodies used: Isolectin GS-IB4 1:200 (#I21412, ThermoFisher Scientific), rabbit anti-mouse Dystrophin 1:200 (#ab15277, Abcam), rabbit anti-Kir4.1 (KCNJ10) antibody (#APC-035, Alomone labs), anti-rat Aqp4 antibody (Aqp41-S, AlphaDiagnostic), mouse anti-Rhodopsin Ab (#MAB 5356, EMD Millipore), anti-rabbit PKCα Ab 1:2000 (P4334, Sigma). Chicken anti-rabbit 488 1:500 (#41221, ThermoFisher), chicken anti-rat 488 (#21470, ThermoFisher) or donkey anti-mouse 488 (#21202, ThermoFisher) were used as secondary Ab.

2.4. Image analysis

Branching index (number of branch points/mm^2) of the vascular plexus was determined in 4 regions of interest (ROI) per retinal flatmount using AngioTool (Zudaire et al., 2011). Normalized Fluorescence Intensity (NFI) of Aqp4 and Kir4.1 in retinal cross-sections was determined using Fiji ImageJ. NFI was calculated as the Integrated Density of the region of interest (ROI) – (Area of the ROI x Mean fluorescence of background). Statistical analysis was performed using GraphPad Prism version 7.0 (GraphPad Software, San Diego, CA).

2.5. Western blot

Total retina lysates were made in T-Per buffer with 1% Protease- and Phosphatase Inhibitor. Samples were resolved in 4–12% NuPAGE Bis-Tris gels (ThermoFisher Scientific) under denaturing conditions and blotted onto polyvinylidene fluoride membranes. Primary antibodies were incubated overnight at 4 °C: rabbit anti-mouse Dystrophin 1:1000 (#ab15277, Abcam), mouse monoclonal anti-bActin Ab (#A1978, Sigma-Aldrich). Secondary antibodies incubated for 1 h at room temperature: IRDye 800CW Donkey anti-Rabbit (#925–32213, Licor), IRDye 680CW Donkey anti-Mouse (#925–68180, Licor). The Odyssey Fc Imaging System was used.

2.6. qPCR

RNA was extracted using the miRNeasy Mini Kit (#217004, Qiagen) and translated into cDNA (QuantiTect Reverse Transcription Kit, #205310, Qiagen). The following primer pairs were used with an annealing temperature of 52 °C or 60 °C: Dp427 for CTTTCAGGAAGATG ACAGAATCAG, Dp427 rev TTGTTCAGGGATGAATTCTTGTA, Dp260 for ATAAGCAAAGCTGAATGAGTGCT, Dp260 rev TTCTTCATTTCTTC TAAACT, Dp140 for GCATTGCTGACTGTTCTGAGC, Dp140 rev CCCA GTTGCATTCAGTGTTCTG, Dp71 ATGAGGGAACACCTCAAAGGCCACG, Dp71 rev TCTGGAGCCTTCTGAGCTTC (Dalloz et al., 2001), bActin for GGCTGTATTCCCCTCCATCG, bActin rev CCAGTTGGTAACAATGCCA TGT, mVEGF120 for GCCAGCACATAGAGAGAATGAGC,mVEGF120rev CGGCTTGTCACATTTTTCTGG, mVEGF164 for GCCAGCACATAGAGA GAATGAGC, mVEGF164 rev CAAGGCTCACAGTGATTTTCTGG, mVEGF188 for GCCAGCACATAGAGAGAATGAGC, mVEGF188 rev AACAAGGCTCACAGTGAACGCT, Kir4.1 for CCGCGATTTATCAGAGC, Kir4.1 rev AGATCCTTGAGGTAGAGGAA, Aqp4 for CTTTCTGGAAGGC AGTCTCAG, Aqp4 rev CCACACCGAGCAAAACAAAGAT, Rhod for TCA TGGTCTTCGGAGGATTCAC, Rhod rev TACACCTCCAAGTGTGGCA AAG, Cone for CAAGCCCTTTGGCAATGTGA, Cone rev GCTCCAACCA AAGATTGGTGG.

2.7. In situ

The Affymetrix QuantiGene View RNA ISH system was used according to the manufacturer's instructions. Briefly, whole eyes were fixed in 4% PFA for 6 h, followed by 24 h of 20% sucrose. Sections were further fixed in 4% formaldehyde at 4 °C for 16 h prior to ISH. Protease solution was applied to eyes (1:25 dilution) for 10 min at 40 °C. Probes were designed and made by Affymetrix using the accession number NM_007868 for Dp427 (VB1-17113).

2.8. Ganzfeld electroretinography (ERG)

ERG's were performed as previously described (Bucher et al., 2017). Mice were dark-adapted overnight. All following procedures were performed under dim red light. Mice received ketamine (60 mg/kg) and xylazine (10 mg/kg) IP. Pupils were dilated with hydroxyamphetamine 0.25%/tropicamide 1%. Signals were recorded from the corneal surface. Electrodes at the forehead and tail served as reference and ground. The Espion E2 Colordome (Diagnosys LLC) was used for stimulation. In

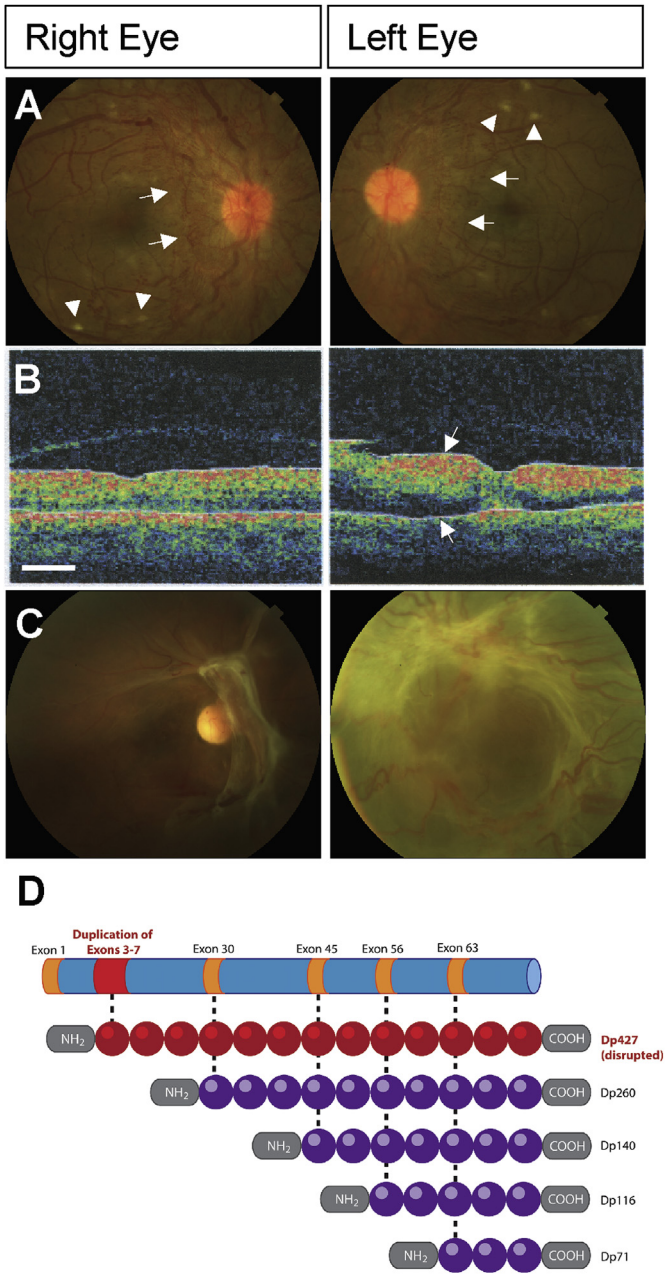

Fig. 1. Vasoproliferative fundus changes in a 21 year-old DMD patient following an anemic crisis. At initial presentation, fundus images revealed abundant neovascular changes (arrows) and cotton wool spots (arrowheads). (B) OCT revealed subretinal fluid in the nasal retina, with an increase up to 524 nm in retinal thickness in the left eye. Scale bar = 1 mm (C) 1 year after initial presentation, pronounced pre-retinal fibrotic changes persisted. (D) MLPA analysis of genomic DNA showed a duplication of exons 3–7 of the dystrophin gene.

the dark-adapted (scotopic) state, white flashes of increasing intensities (1x 10-5 cd s/m^2) were used to record rod and mixed rod/cone responses. Background light of 30 cd s/m^2 was used to light-adapt mice. White flashes (1-Hz, (0.63–20 cd s/m^2) and Flicker stimuli (30-Hz, 3.98, 10, 20 cd s/m^2) were used to measure cone responses.

3. Results

3.1. Severe proliferative retinopathy in a DMD patient with a mutation in Dp427

A 21-year old male DMD patient developed significant pre-retinal neovascularization (arrows) and cotton wool spots (arrow heads) in both eyes (Fig. 1A), which led to a decrease in visual acuity. Medical history included sleep apnea and pulmonary atelectasis, probably in the context of DMD. In response to a continuous decline in visual acuity to counting fingers due to retinal edema over the next two weeks (Fig. 1B), the patient received a single intravitreal injection of anti-VEGF antibody into the left eye (LE). Three weeks afterwards, the patient was hospitalized due to sepsis of unknown origin accompanied by acute renal failure and chronic anemia (hemoglobin of 7.1). Follow-up exams during that time revealed exacerbation of retinal neovascularization in the right eye (RE) and development of massive pre-retinal fibrosis in the LE. The patient received two intravitreal injections of an anti-VEGF agent into the right eye over the next 2 months to treat the increasing retinal neovascularization, while the LE did not receive further injections due to severe fibrotic changes without associated neovascularization or retinal edema. The retinal changes in both eyes finally stabilized after the recovery of overall health status as illustrated in the fundus-photographs taken 1 and 2 years after initial presentation (Fig. 1C, Supplemental Fig. 1).

Since the short dystrophin gene product Dp71 is known to be involved in retinal vascular homeostasis and osmoregulation (Dalloz et al., 2003; El Mathari et al., 2015; Sene et al., 2009), we hypothesized that the patient had a genetic mutation that affected Dp71. Surprisingly, analysis of genomic DNA from blood samples of the patient detected a duplication of exon 3–7 of the dystrophin gene, predicting a major disruption in the expression of the full-length dystrophin gene product Dp427 (Fig. 1D). We thus performed preclinical studies to further evaluate the role of Dp427 in the retina during development and in response to stress, including ageing and hypoxia.

3.2. The mouse retina expresses multiple dystrophin gene products

While most tissues, like muscle (Dp427) or brain (Dp71), predominantly express one dystrophin gene product, the retina expresses multiple gene products at similar levels, including Dp427, Dp260, Dp140 and Dp71 (Fig. 2A). To better understand the role and regulation of the different gene products in the retina, a time course of quantitative PCR and Western Blot analyses during retinal development was performed. Surprisingly, expression of Dp427 and Dp260 significantly increased during retinal development, while Dp71 and Dp140 expression levels remained constant (Fig. 2 B + C). *In situ* analysis was then performed to specifically localize the expression of dystrophin gene products. Confirming previously published data, Dp427 expression was strongly detected in the inner and outer nuclear layer (INL/ONL); attempts to localize Dp71 and Dp260 with *in situ* analysis failed to yield reproducible results (Wersinger et al., 2011). Surprisingly, a clear signal for Dp427 was also detected in the ganglion cell layer (GCL) (Fig. 2D), suggesting that Dp427 may be expressed throughout all retinal layers. Immunohistochemical staining using a pan-dystrophin antibody detected a positive signal in the GCL, IPL and OPL, but did not allow us to distinguish between the single dystrophin gene products. Interestingly, the fluorescent dystrophin signal localized to the perivascular area in the GCL and IPL, while a strong granulated signal was visible in the OPL (Fig. 2E). Differences between the broad expression pattern along the nuclear layers observed by *in situ* hybridization and the rather localized expression of dystrophins seen by immunohistochemistry may be explained by the scaffolding function and microdomain concentration of dystrophins at the protein level.

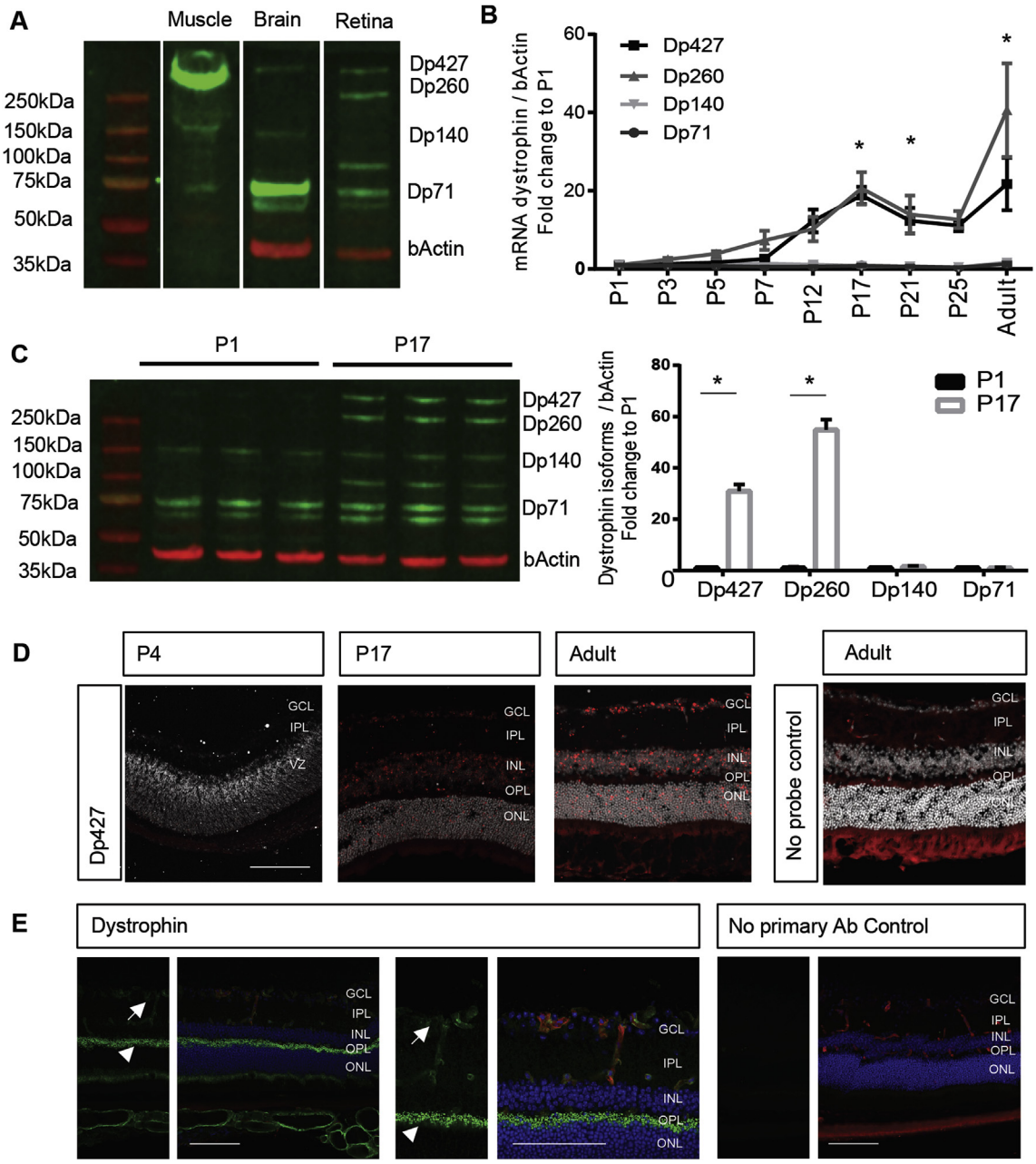

Fig. 2. Temporal and spatial expression patterns of dystrophin gene products in the retina. (A) Western blot analysis of dystrophin gene products shows that the retina expresses at least 4 different dystrophin gene products at similar levels (Dp427, Dp260, Dp140 and Dp71), while brain and muscle tissue predominantly express 1 gene product. Tissues were collected from adult mice. (B) Quantification of dystrophin gene products during retinal development at the RNA level. (N = 4–7 mice per time point) (C) Representative western blot showing biological replicates per lane and quantification results (N = 6 mice per time point) showing that Dp427 and Dp260 are significantly upregulated during maturation, while Dp140 and Dp71 remain unchanged. Error bars represent SEM. Two-way ANOVA: *p < 0.05. (D) In situ analysis on wild-type retinas localizes Dp427 to the ganglion cell, as well as inner and outer nuclear layers. GCL = Ganglion Cell Layer, IPL = Inner Plexiform Layer, VZ = Ventricular Zone, OPL = Outer Plexiform Layer, ONL= Outer Nuclear Layer, Scale bar = 100 μm. (E) Immunohistochemical staining of retinal cross-sections of 8-week-old WT mice with a pan-dystrophin antibody shows a perivascular staining in the GCL and IPL (arrows) as well as strong granular signal in the OPL (arrow head). Scale bars = 100 μm.

3.3. Loss of Dp427 does not affect retinal vascular development

Mdx mice with a point-mutation affecting expression of the long dystrophin gene product Dp427 represent the most common mouse model studied for Duchenne muscular dystrophy. Western blot analysis confirmed that these mice lack Dp427 in the retina, while all other dystrophin gene products were present (Fig. 3A). Vascular development, measured by total vascularized area (Fig. 3B), and branching points (Fig. 3C, Supplemental Fig. 2) were not significantly altered between Mdx mice and wildtype littermate controls (WT). Retinal function in young adult mice (12–16 weeks) showed a significant but relatively small decrease (maximum of 23–26%) in a- and b-wave amplitude under scotopic conditions, while photopic ERG responses remained unaltered (Fig. 3D).

3.4. Retinal function deteriorates in Mdx mice with ageing

In contrast to young mice, aged Mdx mice (15–18 months) presented significantly reduced a-wave (up to 40%) and b-wave (up to 60%) amplitudes, as well as photopic b-wave and peak amplitudes in

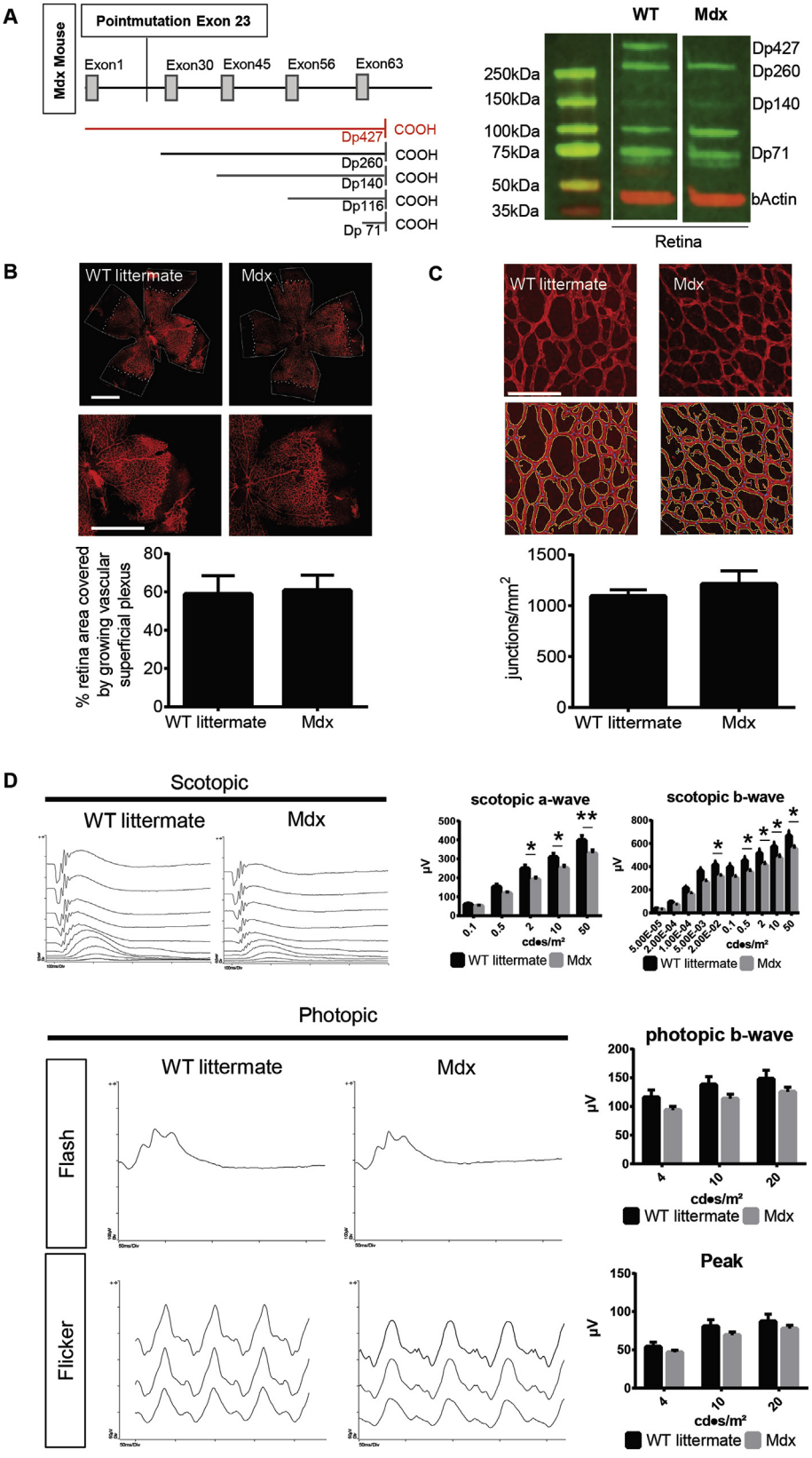

Fig. 3. Defects in Dp427 expression do not affect retinal development. (A) A point mutation in exon 23 leads to lack of Dp427 expression in the retinas of Mdx mice. Western Blot analysis of retinal lysates from adult mice (> 8 weeks). (B) The retinal area that is covered by the growing vascular superficial plexus (in %) at postnatal day 5 (P5) was unchanged in Mdx mice relative to WT littermate controls. (N (WT littermate) = 5, N (Mdx) = 13, error bars represent SEM, Scale bars = 1 mm). (C) Branching index of the superficial plexus was not significantly altered between Mdx and WT littermate controls (N (WT littermate) = 5, N (Mdx) = 5, error bars represent SEM, scale bar = 100 µm). (D) At 12–16 weeks of age, Mdx mice show only minor changes in scotopic a- and b-wave amplitudes and normal photopic ERGs compared to WT littermate controls. (N (WT littermate) = 5, N(Mdx) = 6, repeated measures two-way ANOVA: *p < 0.05, **p < 0.01).

ERG (Fig. 4A). This suggests a worsening of the rod photoreceptor (a-wave) and inner retina (b-wave) function as well as established cone photoreceptor dysfunction at this age. Surprisingly, qPCR analysis did not show significant changes in overall expression levels of photoreceptor markers rhodopsin and opsin or dystrophin-associated channels inward rectifying potassium channel (Kir4.1) and aquaporin 4 (Aqp4) (Supplemental Fig. 3A). To screen for localized expression changes at the protein level, immunohistochemistry was performed on retinal cross-sections of 15-month-old Mdx mice and WT littermate controls. Qualitative as well as semi-quantitative analysis of three Mdx

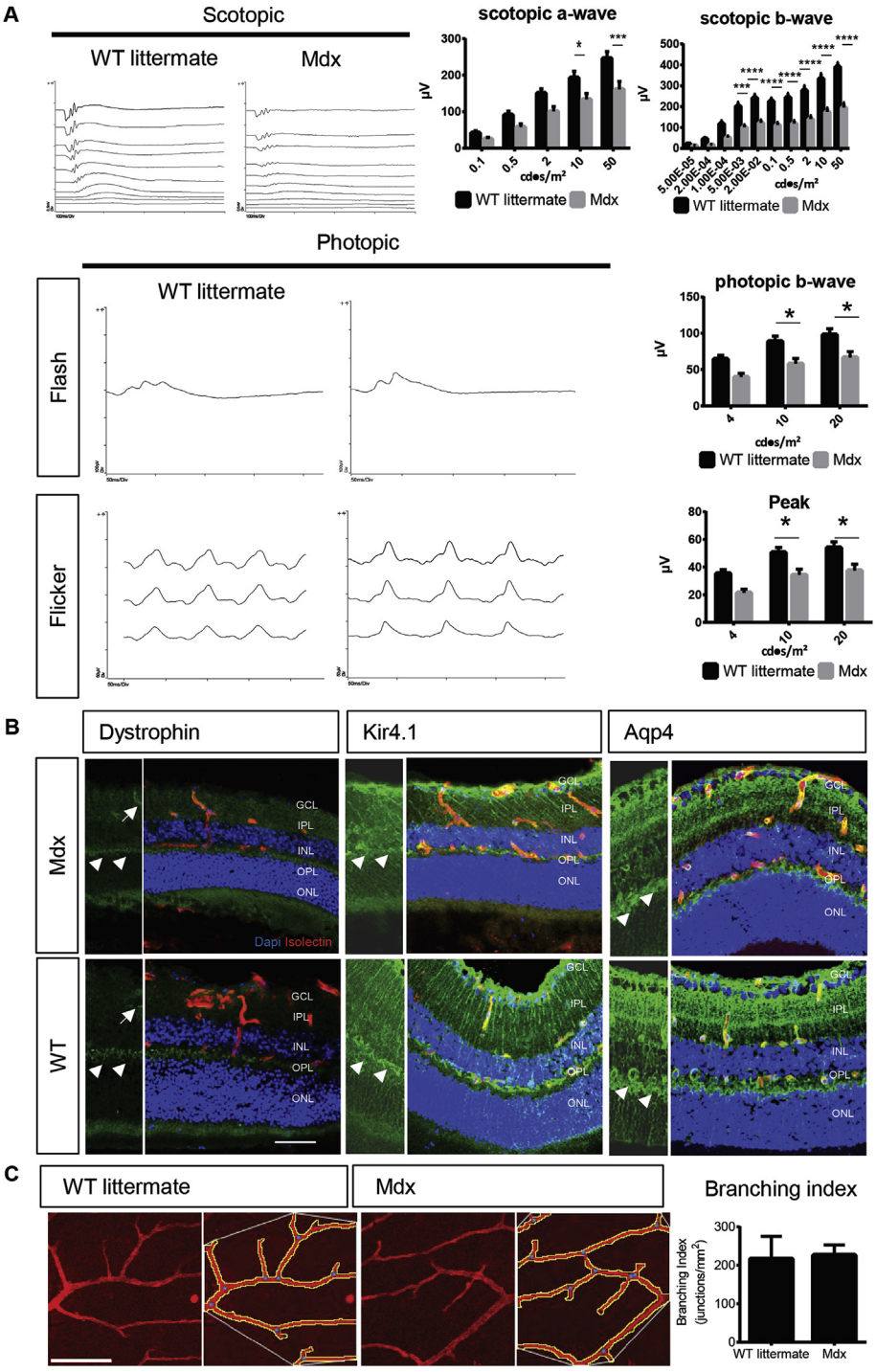

Fig. 4. Lack of Dp427 alters retinal function in aged Mdx mice. (A) At 15 months of age, Mdx mice have significantly reduced scotopic b-waves as well as photopic b-waves and Peak-amplitudes. (N(WT littermate) = 6, N(Mdx) = 11, repeated measures two-way ANOVA: *p < 0.05, **p < 0.01, ***p < 0.001,****p < 0.0001) (B) Representative immunhistochemical stainings of retinal cryosections of Mdx and WT littermate controls with pan-dystrophin, Kir4.1 and Aqp4 antibodies. Arrow heads indicate fluorescent signal in the OPL, arrows paravascular signal (N = 3 mice per group, scale bar = 50 μm). (C) The branching index of the superficial vascular bed is unaltered in aged (15–18 months) Mdx mice compared to WT littermate controls. (N(WT littermate) = 3, N(Mdx) = 7, scale bar = 100 μm).

mice and controls following ERG revealed only slight morphological alterations (Fig. 4B, Supplemental Figs. 3B and C). Using a panspecific dystrophin antibody, immunofluorescence showed a less granulated signal in the OPL (arrow heads) in Mdx mice compared to WT littermate controls (Fig. 4B), suggesting that the granulated signal originates from Dp427 as well as other dystrophin gene products. However, semi-quantitative analysis of the fluorescent dystrophin signal was not possible due to the overall faint signal. Kir4.1, a potassium channel known to associate with the Dp71-glycoprotein complex in Müller cells (Connors et al., 2004), appeared to be expressed at lower levels in the OPL while semi-quantitative analysis of the fluorescence signal failed to reach statistical significance (N = 3; Supplemental Fig. 3C). Staining for Aqp4, a type-4 water-permeable channel known to be connected to the dystrophin-glycoprotein complex (Frigeri et al., 1998), also showed a trend toward localized decrease of signal in the inner retina (OPL to GCL) but not OPL in Mdx mice compared to controls, although this did not reach statistical significance. Despite the functional changes seen in ERG, bipolar cell (labeled by PKCα) and rod photoreceptor (labeled by rhodopsin) expression patterns appeared unchanged between Mdx mice and controls (Supplemental Figs. 3A and B). Analysis of the branching points of the superficial vascular bed also did not demonstrate secondary changes in the retinal vascular bed in aged Mdx mice (Fig. 4C).

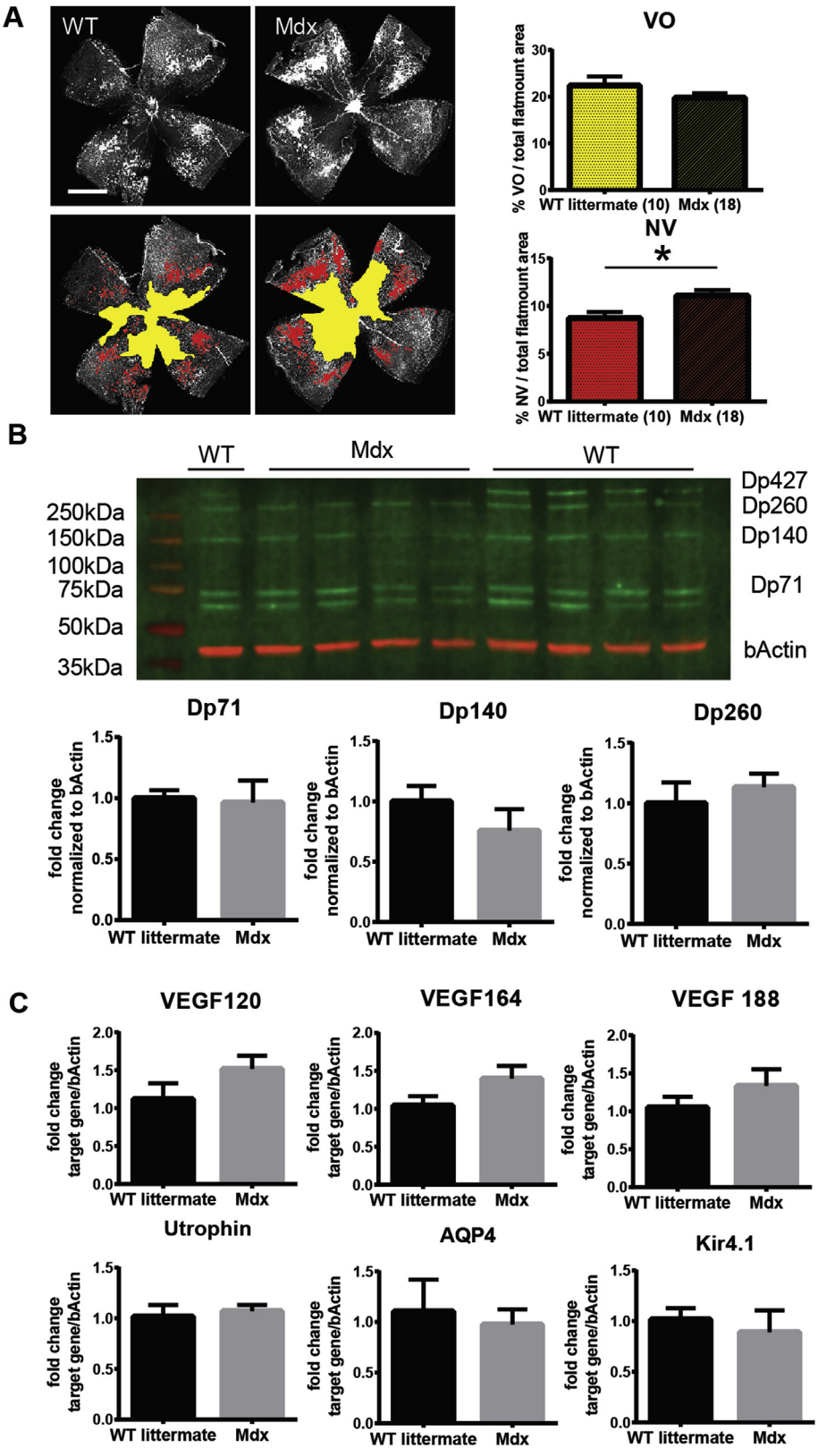

Fig. 5. Defects in Dp427 increase pathological neovascularization in response to retinal hypoxia. (A) Mdx mice with defective expression of Dp427 develop significantly more pre-retinal tufts compared to WT littermate controls (N(WT littermate) = 10, N(Mdx) = 18, Mann-Whitney: *p < 0.05). Area of vaso-obliteration (VO) outlined in yellow, area of neovascularization (NV) outlined in red. (B) At OIR P14, western blot of total retina lysates of Mdx and WT littermate controls (N = 4–5 mice, Mann-Whitney test: *p < 0.05) show no signs of a compensatory upregulation of dystrophin gene products in the absence of Dp427. In the presented WB, each lane represents a biological replicate. (C) qPCR analysis of all three VEGF isoforms, Utrophin, Kir4.1 and Aqp4 at OIR P14 shows no significant change in Mdx mice. (N(WT littermate) = 7 mice, N (MDX) = 7), Mann-Whitney test:*y < 0.05).

3.5. Mdx mice develop excessive pre-retinal neovascularization in response to hypoxia

In our clinical case, retinal hypoxia due to late-stage complications of DMD was likely a stress factor. We thus chose the model of oxygen-induced retinopathy (OIR) to mimic retinal ischemia. In this model, Mdx mice developed significantly more pre-retinal neovascularization compared to their WT littermate controls (Fig. 5A). Results also showed that the VO area tended to be smaller in Mdx mice, although results failed to reach statistical significance. Western blot analysis confirmed that loss of Dp427 was not compensated by upregulation of other dystrophin gene products in OIR (Fig. 5B). Utrophin, an autosomal

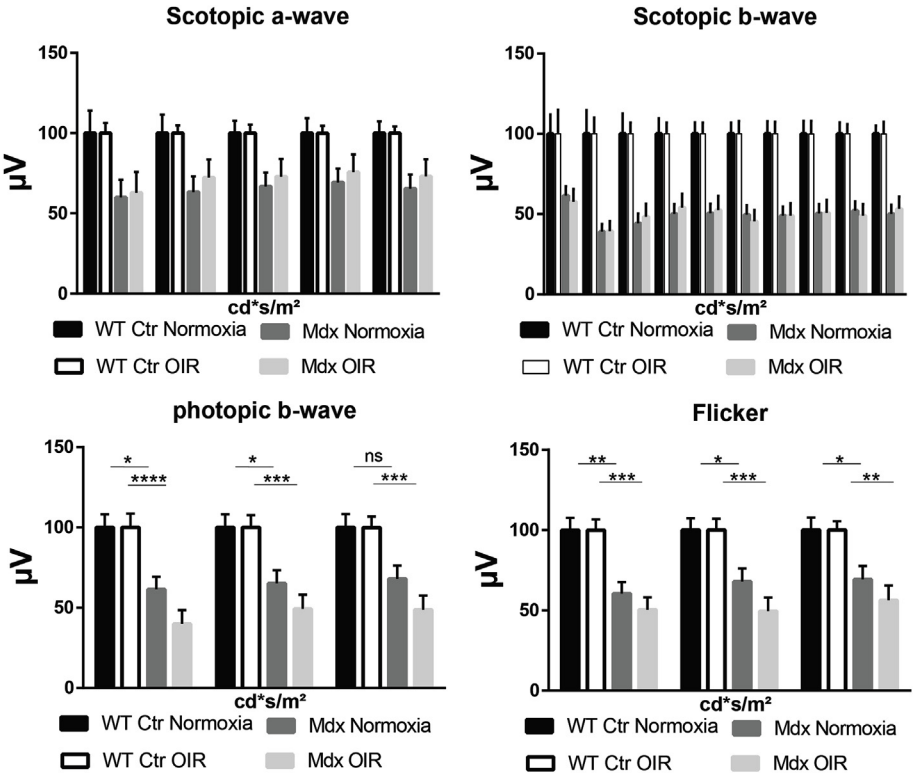

Fig. 6. Temporary retinal hypoxia enhances the deterioration of cone photoreceptor function in aged Mdx mice. ERG analyses of 15-month-old Mdx mice and WT littermate controls that have been exposed to the OIR model show a greater decrease in photopic b-wave and Peak amplitudes than age-matched adults. Mdx Normoxia was normalized to WT control (Ctr) Normoxia and Mdx OIR was normalized to WT Ctr OIR (N(WT Ctr Normoxia) = 6 mice, N(Mdx Normoxia) = 11 mice, N(WT Ctr OIR) = 8 mice, N(Mdx OIR) = 8 mice, repeated measures two-way ANOVA; *p < 0.05, **p < 0.01, ***p < 0.005, **** < 0.0001.

analog of dystrophin that can form a complex with components of the dystrophin-dystroglycan complex (Claudepierre et al., 2000), was also not upregulated at OIR P14, as shown by qPCR analysis (Fig. 5C). Likewise, expression levels of VEGF isoforms as well as Kir4.1 and Aqp4 remained unaltered in Mdx mice at OIR P14.

3.6. *Transient hypoxia enhances deterioration of retinal function in aged Mdx mice*

Analyses of retinal vascular morphology at OIR P17 showed that Mdx mice are more susceptible to hypoxic stress than WT littermate controls. However, the vascular changes observed in OIR are temporary. Long-term studies have previously shown that retinal function following OIR fully recovers in wildtype mice (Nakamura et al., 2012). Thus, we investigated whether Mdx mice are not only prone to temporary vascular changes, but also long-lasting functional alterations following transient hypoxic stress. In our ERG studies, the decrease in photopic b-wave amplitudes and Flicker amplitudes was greater in aged Mdx mice following OIR compared to the observed decrease in Mdx mice not exposed to OIR (Fig. 6). Data were normalized to WT mice following normal development (Normoxia) or OIR to account for the functional changes observed in Mdx mice due to the ageing process alone (Fig. 4). Despite the observed functional changes in aged Mdx mice following transient hypoxia, qPCR and IHC on retinal cross-sections of these mice did not reveal significant alterations (data not shown).

Taken together, these data suggest that transient hypoxia at an early age not only induces temporary morphological, but also long-lasting functional, changes in Mdx mice compared to WT controls. Lack of Dp427 appears to make the retina susceptible to stressors like ageing and hypoxia, and our findings suggest that theses stressors can co-operate to exacerbate the retinal phenotype in dystrophin-deficient subjects.

4. Discussion

To date, four other clinical cases of DMD patients with proliferative retinopathy have been published (Fagan et al., 2012; Hahn et al., 2013; Louie et al., 2004; So et al., 2012). In all cases, DMD patients were older than 20-years and suffered from cardiomyopathy and respiratory problems. The correlation between insufficient oxygenation and vasoproliferative retinal changes in all cases strongly suggested that mutations in the dystrophin gene predisposes patients to development of hypoxia-induced neovascularization. While the impact of Dp71 on retinal function and angiogenesis is well established (Dalloz et al., 2003; Howard et al., 1998), genetic analysis of the patient described in our case report suggested that defects in the full-length dystrophin gene product Dp427 may be associated with vasoproliferative changes in patients with peripheral tissue hypoxia. In the literature, only one out of the four published case reports described genetic testing to further characterize the mutation causing DMD (Hahn et al., 2013). In that case, a deletion affecting exon 8 through 29 was identified, supporting our observation that a defect in Dp427 expression was associated with vasoproliferative retinopathy.

Based on these clinical observations, we hypothesized that lack of Dp427 alters retinal homeostasis and predisposes DMD patients to retinal complications. This hypothesis is supported by our data that show (1) normal retinal development (Fig. 3B) but deterioration of visual function in aged Mdx mice (Fig. 4A) and (2) excessive neovascularization in response to retinal ischemia (Fig. 5A). DMD patients are known to demonstrate normal retinal vasculature and normal visual acuity, but abnormal retinal function on ERG (Cibis et al., 1993; Fitzgerald et al., 1994; Pillers et al., 1993). Extensive ERG studies in men and mice have revealed that the alterations in retinal function depend on the localization of the mutation and lack of specific dystrophin gene products (D'Souza et al., 1995; Kameya et al., 1997; Pillers et al., 1999a; Pillers et al., 1999b; Pillers et al., 1995; Ricotti et al., 2016; Sigesmund et al., 1994). Focusing on the role of Dp427, some early studies suggested that mutations upstream of exon 30 did not lead to changes in ERG in humans or mice (Pillers et al., 1999b; Sigesmund

et al., 1994) while other studies revealed that these patients have decreased a:b ratios compared to healthy controls. (Fitzgerald et al., 1994; Ricotti et al., 2016). Our ERG data of young adult Mdx mice suggested mild, but statistically significant, changes in scotopic a- and b-wave amplitudes compared to WT littermate controls (Fig. 3C). The differences between our study results and that of Pillers et al. (1999b), who detected normal ERG amplitudes in 20-week-old Mdx mice, may be explained by the more sensitive ERG technology available today compared to the technology used in 1999. Furthermore, in our study Mdx mice were compared to WT littermate controls with the background of C57BL/10ScSn-*Dmd*^{mdx}/J, while the previous studies used mice on a C57BL/6J background.

Interestingly, scotopic and photopic retinal responses in ERG further declined in aged Mdx mice (Fig. 4A), suggesting that Dp427 plays a role in retinal homeostasis during ageing. Unfortunately, there are currently no clinical ERG studies published that confirm our observation in humans, since most clinical studies have included younger patients (< 20 years). Loss of Dp427 may continuously destabilize the retina in the process of ageing and make it more susceptible to additional stressors, like hypoxia. Previous electrophysiological and immunohistochemical studies have already provided strong evidence that Dp427 is expressed in photoreceptor and bipolar cells (Fitzgerald et al., 1994; Pillers et al., 1999a; Wersinger et al., 2011). Dp427 may therefore play a role in formation of the first synapse. These facts correlate well with our observation that Dp427 is strongly upregulated around P17 (Fig. 2B + C), an important time for photoreceptor maturation. Furthermore, it seems reasonable that loss of Dp427 might lead to impairment of the first synapse, which could be represented by reduced a- and b-wave amplitudes in ERG. However, it remains unclear why retinal function is only slightly affected at a young age and deteriorates with aging. Altered expression patterns of dystrophin-dystroglycan associated proteins like Kir4.1 and Aqp4 may present a first step in understanding these functional changes (Fig. 4B). Further studies are necessary to confirm the clinical relevance of our observations and elucidate the underlying molecular mechanisms.

The OIR model was originally developed to mimic retinopathy of prematurity (Smith et al., 1994) and remains one of the most commonly used models to study neovascular changes in response to hypoxic stress (Stahl et al., 2010a, 2010b). In this model, newborn pups with an immature retinal vascular system are exposed to extreme conditions that subsequently cause intraretinal hypoxia (Scott and Fruttiger, 2009). Thus, the OIR model may not well represent the physiology of an aged retina like our clinical case, where synapses as well as the blood-retinal barrier are fully matured. Our observation that Mdx mice develop significantly more neovascularization in the OIR model (Fig. 5A) can, rather, be understood as a way to demonstrate that loss of Dp427 may increase susceptibility of the retina to hypoxia and result in vascular abnormalities under extreme conditions.

While the concept of Dp427 being associated with vascular homeostasis is novel in the retina, multiple studies have highlighted vascular changes in muscular and cerebral tissue of Mdx mice (Ennen et al., 2013; Nico et al., 2003; Shimizu-Motohashi and Asakura, 2014). Straino et al. showed in their preclinical work that arteriogenesis was enhanced in Mdx mice following ischemia as well as in wound healing. The idea of enhanced angiogenesis in response to ischemia in Mdx mice may explain the increase in NV as well as the potentially smaller VO observed in this study. Another hypothesis builds on the observations made by Nico et al., who reported that aged Mdx mice lost integrity of the blood-brain barrier due to changes in vascular endothelial cells as well as swollen glial cells (Nico et al., 2003). Loss of Dp427 in smooth muscle decreases NO-mediated vasodilation and induces functional ischemia, which promotes muscle fiber necrosis in the context of increased susceptibility to metabolic stress (Loufrani et al., 2001; Rando, 2001; Sander et al., 2000). Translating this hypothesis to the retina, loss of Dp427 in vascular smooth muscle cells may exacerbate hypoxia during OIR. In the context of unchanged metabolic demand due to intact retinal function, this exacerbated hypoxia may result in increased neovascularization. Further research is necessary to explore these hypotheses.

5. Conclusions

While the mechanisms underlying our observation that defects in Dp427 can trigger deterioration in retinal function and excessive retinal neovascularization remain elusive, our study has unequivocal clinical implications. DMD patients with mutations in the 5' region of the dystrophin gene should be screened for vasoproliferative retinopathy when they suffer from cardio-respiratory insufficiency that could lead to hypoxia in peripheral organs. Since life expectancy and concomitant cardiovascular complications in DMD patients have significantly increased in recent years, we expect the incidence of Duchenne-associated proliferative retinopathy to also increase. Thus, it is important that these patients be under ophthalmologic surveillance to detect and treat neovascular changes at early stages in order to preserve vision.Acknowledgements

We thank Sarah Harkins-Perry and Maki Kitano for excellent technical support.

Conflicts of interest

No conflicts of interest were declared.

Funding

This work was supported by grants to MF from the National Eye Institute of the National Institutes of Health (EY11254) and the Lowy Medical Research Institute. FB was supported by a fellowship from the German Research Foundation (BU 3135/1-1). MSHF was supported by fellowships from the Howard Hughes Medical Research Institute's Medical Research Fellows Program and the Knight-Hennessy Scholars Program at Stanford University.

Appendix A. Supplementary data

Supplementary data to this article can be found online at https://doi.org/10.1016/j.neuint.2019.104489.

Statement of author contributions

FB, TUK, TK and MF designed and carried out experiments. MSHF, EA and YU carried out experiments and analyzed data. FB, MSHF and MF drafted the manuscript. All authors were involved in writing the paper and had final approval of the submitted and published manuscript.

References

Banin, E., Dorrell, M.I., Aguilar, E., Ritter, M.R., Aderman, C.M., Smith, A.C.H., Friedlander, J., Friedlander, M., 2006. T2-TrpRS inhibits preretinal neovascularization and enhances physiological vascular regrowth in OIR as assessed by a new method of quantification. Invest Ophthalmol Vis Sci 47, 2125–2134.

Bucher, F., Zhang, D., Aguilar, E., Sakimoto, S., Diaz-Aguilar, S., Rosenfeld, M., Zha, Z., Zhang, H., Friedlander, M., Yea, K., 2017. Antibody-mediated inhibition of Tspan12 ameliorates vasoproliferative retinopathy through suppression of beta-catenin signaling. Circulation 136, 180–195.

Byers, T.J., Lidov, H.G., Kunkel, L.M., 1993. An alternative dystrophin transcript specific to peripheral nerve. Nat. Genet. 4, 77–81.

Cibis, G.W., Fitzgerald, K.M., Harris, D.J., Rothberg, P.G., Rupani, M., 1993. The effects of dystrophin gene mutations on the ERG in mice and humans. Invest Ophthalmol Vis Sci 34, 3646–3652.

Claudepierre, T., Dalloz, C., Mornet, D., Matsumura, K., Sahel, J., Rendon, A., 2000. Characterization of the intermolecular associations of the dystrophin-associated glycoprotein complex in retinal Muller glial cells. J. Cell Sci. 113 Pt 19, 3409–3417.

Connor, K.M., Krah, N.M., Dennison, R.J., Aderman, C.M., Chen, J., Guerin, K.I., Sapieha, P., Stahl, A., Willett, K.L., Smith, L.E., 2009. Quantification of oxygen-induced retinopathy in the mouse: a model of vessel loss, vessel regrowth and pathological

angiogenesis. Nat. Protoc. 4, 1565–1573.
Connors, N.C., Adams, M.E., Froehner, S.C., Kofuji, P., 2004. The potassium channel Kir4.1 associates with the dystrophin-glycoprotein complex via alpha-syntrophin in glia. J. Biol. Chem. 279, 28387–28392.
D'Souza, V.N., Nguyen, T.M., Morris, G.E., Karges, W., Pillers, D.A., Ray, P.N., 1995. A novel dystrophin isoform is required for normal retinal electrophysiology. Hum. Mol. Genet. 4, 837–842.
Dalloz, C., Claudepierre, T., Rodius, F., Mornet, D., Sahel, J., Rendon, A., 2001. Differential distribution of the members of the dystrophin glycoprotein complex in mouse retina: effect of the mdx3Cv mutation. Mol. Cell. Neurosci. 17, 908–920.
Dalloz, C., Sarig, R., Fort, P., Yaffe, D., Bordais, A., Pannicke, T., Grosche, J., Mornet, D., Reichenbach, A., Sahel, J., Nudel, U., Rendon, A., 2003. Targeted inactivation of dystrophin gene product Dp71: phenotypic impact in mouse retina. Hum. Mol. Genet. 12, 1543–1554.
El Mathari, B., Sene, A., Charles-Messance, H., Vacca, O., Guillonneau, X., Grepin, C., Sennlaub, F., Sahel, J.A., Rendon, A., Tadayoni, R., 2015. Dystrophin Dp71 gene deletion induces retinal vascular inflammation and capillary degeneration. Hum. Mol. Genet. 24, 3939–3947.
Ennen, J.P., Verma, M., Asakura, A., 2013. Vascular-targeted therapies for Duchenne muscular dystrophy. Skelet Muscle 3, 9.
Fagan, X.J., Levy, J., Al-Qureshi, S., Harper, C.A., 2012. Proliferative retinopathy in Duchenne muscular dystrophy and its response to bevacizumab. Clin. Exp. Ophthalmol. 40, 906–907.
Fitzgerald, K.M., Cibis, G.W., Giambrone, S.A., Harris, D.J., 1994. Retinal signal transmission in Duchenne muscular dystrophy: evidence for dysfunction in the photoreceptor/depolarizing bipolar cell pathway. J. Clin. Investig. 93, 2425–2430.
Frigeri, A., Nicchia, G.P., Verbavatz, J.M., Valenti, G., Svelto, M., 1998. Expression of aquaporin-4 in fast-twitch fibers of mammalian skeletal muscle. J. Clin. Investig. 102, 695–703.
Hahn, P., Lin, P., Fekrat, S., 2013. Ultra-widefield imaging of Duchenne muscular dystrophy-associated proliferative retinal vasculopathy improved with panretinal laser photocoagulation alone. Ophthalmic Surg Lasers Imaging Retina 44, 293–295.
Howard, P.L., Dally, G.Y., Wong, M.H., Ho, A., Weleber, R.G., Pillers, D.A., Ray, P.N., 1998. Localization of dystrophin isoform Dp71 to the inner limiting membrane of the retina suggests a unique functional contribution of Dp71 in the retina. Hum. Mol. Genet. 7, 1385–1391.
Kameya, S., Araki, E., Katsuki, M., Mizota, A., Adachi, E., Nakahara, K., Nonaka, I., Sakuragi, S., Takeda, S., Nabeshima, Y., 1997. Dp260 disrupted mice revealed prolonged implicit time of the b-wave in ERG and loss of accumulation of beta-dystroglycan in the outer plexiform layer of the retina. Hum. Mol. Genet. 6, 2195–2203.
Lederfein, D., Levy, Z., Augier, N., Mornet, D., Morris, G., Fuchs, O., Yaffe, D., Nudel, U., 1992. A 71-kilodalton protein is a major product of the Duchenne muscular dystrophy gene in brain and other nonmuscle tissues. Proc. Natl. Acad. Sci. U. S. A. 89, 5346–5350.
Lidov, H.G., Selig, S., Kunkel, L.M., 1995. Dp140: a novel 140 kDa CNS transcript from the dystrophin locus. Hum. Mol. Genet. 4, 329–335.
Loufrani, L., Matrougui, K., Gorny, D., Duriez, M., Blanc, I., Levy, B.I., Henrion, D., 2001. Flow (shear stress)-induced endothelium-dependent dilation is altered in mice lacking the gene encoding for dystrophin. Circulation 103, 864–870.
Louie, K., Apte, R.S., Mori, K., Gehlbach, P., 2004. Severe proliferative retinopathy in a patient with advanced muscular dystrophy. Br. J. Ophthalmol. 88, 1604–1605.
Muntoni, F., Torelli, S., Ferlini, A., 2003;al.,. Dystrophin and mutations: one gene, several proteins, multiple phenotypes. Lancet Neurol. 2, 731–740.
Nakamura, S., Imai, S., Ogishima, H., Tsuruma, K., Shimazawa, M., Hara, H., 2012. Morphological and functional changes in the retina after chronic oxygen-induced retinopathy. PLoS One 7, e32167.
Nico, B., Frigeri, A., Nicchia, G.P., Corsi, P., Ribatti, D., Quondamatteo, F., Herken, R., Girolamo, F., Marzullo, A., Svelto, M., Roncali, L., 2003. Severe alterations of endothelial and glial cells in the blood-brain barrier of dystrophic mdx mice. Glia 42, 235–251.
Pillers, D.A., Bulman, D.E., Weleber, R.G., Sigesmund, D.A., Musarella, M.A., Powell, B.R., Murphey, W.H., Westall, C., Panton, C., Becker, L.E., et al., 1993. Dystrophin expression in the human retina is required for normal function as defined by electroretinography. Nat. Genet. 4, 82–86.
Pillers, D.A., Fitzgerald, K.M., Duncan, N.M., Rash, S.M., White, R.A., Dwinnell, S.J., Powell, B.R., Schnur, R.E., Ray, P.N., Cibis, G.W., Weleber, R.G., 1999a. Duchenne/Becker muscular dystrophy: correlation of phenotype by electroretinography with sites of dystrophin mutations. Hum. Genet. 105, 2–9.
Pillers, D.A., Weleber, R.G., Green, D.G., Rash, S.M., Dally, G.Y., Howard, P.L., Powers, M.R., Hood, D.C., Chapman, V.M., Ray, P.N., Woodward, W.R., 1999b. Effects of dystrophin isoforms on signal transduction through neural retina: genotype-phenotype analysis of duchenne muscular dystrophy mouse mutants. Mol. Genet. Metab. 66, 100–110.
Pillers, D.A., Weleber, R.G., Woodward, W.R., Green, D.G., Chapman, V.M., Ray, P.N., 1995. mdxCv3 mouse is a model for electroretinography of Duchenne/Becker muscular dystrophy. Invest Ophthalmol Vis Sci 36, 462–466.
Rando, T.A., 2001. Role of nitric oxide in the pathogenesis of muscular dystrophies: a "two hit" hypothesis of the cause of muscle necrosis. Microsc. Res. Tech. 55, 223–235.
Ricotti, V., Jagle, H., Theodorou, M., Moore, A.T., Muntoni, F., Thompson, D.A., 2016. Ocular and neurodevelopmental features of Duchenne muscular dystrophy: a signature of dystrophin function in the central nervous system. Eur. J. Hum. Genet. 24, 562–568.
Romitti, P.A., Zhu, Y., Puzhankara, S., James, K.A., Nabukera, S.K., Zamba, G.K., Ciafaloni, E., Cunniff, C., Druschel, C.M., Mathews, K.D., Matthews, D.J., Meaney, F.J., Andrews, J.G., Conway, K.M., Fox, D.J., Street, N., Adams, M.M., Bolen, J., 2015. Prevalence of duchenne and becker muscular dystrophies in the United States. Pediatrics 135, 513–521.
Sander, M., Chavoshan, B., Harris, S.A., Iannaccone, S.T., Stull, J.T., Thomas, G.D., Victor, R.G., 2000. Functional muscle ischemia in neuronal nitric oxide synthase-deficient skeletal muscle of children with Duchenne muscular dystrophy. Proc. Natl. Acad. Sci. U. S. A. 97, 13818–13823.
Scott, A., Fruttiger, M., 2009. Oxygen-induced retinopathy: a model for vascular pathology in the retina. Eye 24, 416–421.
Sene, A., Tadayoni, R., Pannicke, T., Wurm, A., El Mathari, B., Benard, R., Roux, M.J., Yaffe, D., Mornet, D., Reichenbach, A., Sahel, J.A., Rendon, A., 2009. Functional implication of Dp71 in osmoregulation and vascular permeability of the retina. PLoS One 4, e7329.
Shimizu-Motohashi, Y., Asakura, A., 2014. Angiogenesis as a novel therapeutic strategy for Duchenne muscular dystrophy through decreased ischemia and increased satellite cells. Front. Physiol. 5, 50.
Sigesmund, D.A., Weleber, R.G., Pillers, D.A., Westall, C.A., Panton, C.M., Powell, B.R., Heon, E., Murphey, W.H., Musarella, M.A., Ray, P.N., 1994. Characterization of the ocular phenotype of Duchenne and Becker muscular dystrophy. Ophthalmology 101, 856–865.
Smith, L.E., Wesolowski, E., McLellan, A., Kostyk, S.K., D'Amato, R., Sullivan, R., D'Amore, P.A., 1994. Oxygen-induced retinopathy in the mouse. Invest Ophthalmol Vis Sci 35, 101–111.
So, K., Shinoda, K., Watanabe, E., Mashiko, T., Mizota, A., 2012. VITRECTOMY FOR PROLIFERATIVE RETINOPATHY IN PATIENT WITH ADVANCED DUCHENNE MUSCULAR DYSTROPHY. Retin. Cases Brief Rep. 6, 142–144.
Stahl, A., Chen, J., Sapieha, P., Seaward, M.R., Krah, N.M., Dennison, R.J., Favazza, T., Bucher, F., Lofqvist, C., Ong, H., Hellstrom, A., Chemtob, S., Akula, J.D., Smith, L.E., 2010a. Postnatal weight gain modifies severity and functional outcome of oxygen-induced proliferative retinopathy. Am. J. Pathol. 177, 2715–2723.
Stahl, A., Connor, K.M., Sapieha, P., Chen, J., Dennison, R.J., Krah, N.M., Seaward, M.R., Willett, K.L., Aderman, C.M., Guerin, K.I., Hua, J., Lofqvist, C., Hellstrom, A., Smith, L.E., 2010b. The mouse retina as an angiogenesis model. Invest Ophthalmol Vis Sci 51, 2813–2826.
Wersinger, E., Bordais, A., Schwab, Y., Sene, A., Benard, R., Alunni, V., Sahel, J.A., Rendon, A., Roux, M.J., 2011. Reevaluation of dystrophin localization in the mouse retina. Invest Ophthalmol Vis Sci 52, 7901–7908.
Zudaire, E., Gambardella, L., Kurcz, C., Vermeren, S., 2011. A computational tool for quantitative analysis of vascular networks. PLoS One 6, e27385.